International Journal of Engineering Research & Technology (IJERT)
ISSN: 2278-0181
Vol. 9 Issue 11, November-2020

The Impact of Climate Change on the Water Quality of Ground Water in Limbe-Cameroon

Fonteh Mathias Fru[1] and Motchemien Rigobert[2]*
[1] College of Technology, The University of Bamenda, Box 39, Bambilli, Mezam Division, NW Region, Cameroon.
[2] Department of Rural Engineering, National Advanced School of Public Works Buea, Box 324 Buea, SW Region, Cameroon.

Abstract:- **A significant proportion of the population of Limbe, a coastal town in Cameroon, relies on ground water (gw) to satisfy their drinking water needs. The coastal aquifer is threatened by pollution from sea water intrusion and hence the aim of this study was to determine the suitability of the water. Physico-chemical analysis were carried out on samples collected from the study area and the Revelle Index was calculated and used to determine the extent of pollution from seawater intrusion. The water quality index (WQI) was calculated using values of the pH, bicarbonate, chloride, total dissolved solids and the electrical conductivity. The results showed that the sea level rise is projected to rise by 32 cm in 2050 and 82 cm in 2100 due to climate change from 2018; the base year. About 23% of the groundwater in the study area is currently slightly polluted by seawater intrusion. By 2050, this is projected to increase to 30.8 % and to 42.31 % in 2100 due to sea level rise resulting from climate change. About 34.4 % of the ground water in the study area is currently good for drinking while 65.6 % is either poor, very poor or unsuitable for drinking. By 2050, it is projected that the proportion of the ground water considered to be good for drinking will reduce to 26.92 % and down to 17.86 % in 2100. In order to reduce the intrusion of sea water into the aquifer, a halophyte plant like mangrove should be planted at the mouth of the main river in Limbe.**

Keywords: Coastal aquifer, pollution, Revelle Index, salinity, sea level rise, seawater intrusion, water quality index.

I. INTRODUCTION

In the last few decades, there has been a tremendous increase in the demand for fresh water in the world due to the rapid growth of the population and the accelerated pace of industrialization [1]. Limbe, a coastal town in Cameroon on the Atlantic Ocean has a demand for domestic water supply that the water utility company cannot satisfy and hence a significant proportion of the population relies on ground water (gw) to meet their domestic water demands.

Under natural conditions, coastal aquifers are recharged by rainfall, and the gw flows towards the ocean, preventing salt water intrusion into the freshwater. The global mean sea level (GMSL) increased by an average rate of 1.8 mm/year during the 20th century [2] and the IPCC reported with a high confidence that this rate has been increasing [3]. Reference [4] estimated that the GMSL increased by 3.1 mm/year from 1993 to 2003, but this change is not spatially uniform worldwide. Reference [5] estimated a GMSL rise of approximately 3.3 mm/year for the period 1992 to 2010.

He [6] estimated on the basis of data obtained from the tide gauge installed in Limbe, a rise in the mean sea level of the Atlantic Ocean in the lower part of the Gulf of Guinea of about 10 mm / year. One effect of such an increase is sea water intrusion into coastal aquifers [7]. Salt water intrusion is a serious problem because about 80% of the world's population lives along the coast and utilize coastal aquifers for domestic water supply. In addition, over exploitation of coastal aquifers has resulted in falling groundwater levels (gwl). Sea level rise and falling gwl have resulted in increased pollution of gw due to sea water intrusion. This has caused wells previously used for domestic water supply to be abandoned. For example, in New Jersey, more than 120 wells were abandoned because of salt water contamination [8]. In the study area, about 250 wells have been abandoned because the water has become salty [6].

Variations in the sea level and the associated wedge movement can influence the near-shore and/or large-scale submarine discharge patterns and impact nutrient loading levels across the aquifer-ocean interface [9]. While anthropogenic activities, such as over pumping and felling of trees in urbanized coastal areas, are the major causes of salt water intrusion, it is projected that increases in the sea level due to climate change (CC) would aggravate the problem [9]. Reference [10] modelled the impacts of climate change and changes in land use patterns on the salt distribution in a coastal aquifer and concluded that rising sea level could induce rapid progression of salt water intrusion.

Excessive groundwater withdrawals have been reported to result in changes in the physical, chemical and microbiological water quality; drop in the water table level; reverse hydraulic gradient and consequently water quality deterioration in coastal areas [11]. Poor water quality results in incidences of water borne diseases and consequently reduces the life expectancy of the population [12]. Thus, concern for clean and safe drinking water and protection from contamination is justified because a large proportion of the population in the study area depends on ground water for domestic purposes.

Water quality evaluation is based on the physical, chemical and biological parameters ascertaining the suitability for various uses such as domestic consumption, agricultural, recreational and industrial use [13]. The traditional assessment of water quality consists of comparing the point values of water quality parameters levels with their guideline or standard values based on allocated water use or uses. This type of assessment does not provide an overall assessment of water quality of a water body which is important for managers and decision-makers. To resolve this decision-making problem, several water quality indices have been developed to transform point value water quality parameters into integrated indicator values. Many studies have demonstrated the usefulness of assessing the water quality of gw using a water quality index (WQI). Examples are presented by: [14]; [15]; [16]; [17]; [18]; [19]; [20]; and [21].

(This work is licensed under a Creative Commons Attribution 4.0 International License.)

International Journal of Engineering Research & Technology (IJERT)
ISSN: 2278-0181
Vol. 9 Issue 11, November-2020

The aim of this study was to assess the suitability of the gw in Limbe for domestic use in a changing climate specifically to determine the effect of climate change on the sea water intrusion in Limbe; evaluate the change in the extent of sea water intrusion into the aquifer due to climate change; determine the change in the proportion of the gw suitable for drinking due to climate change and propose a solution to reduce the impact of sea water intrusion on the gw quality in the coastal aquifer.

II. MATERIALS AND METHODS

A. The study area

(i) Location

Limbe is located along the coastal area of Fako Division, South-West Region of Cameroon (Figure 1). The study area is located approximately between latitudes 3° 90′ and 4° 05 N and longitudes 9° 29′ and 9° 06′ E. It is bounded in the East by Bimbia, in the North by Bonadikombo, in the South by the Atlantic Ocean and in the West by Mukundange. The population of Limbe is about 130,000 inhabitants spread over a surface area of 596 km^2 [22].

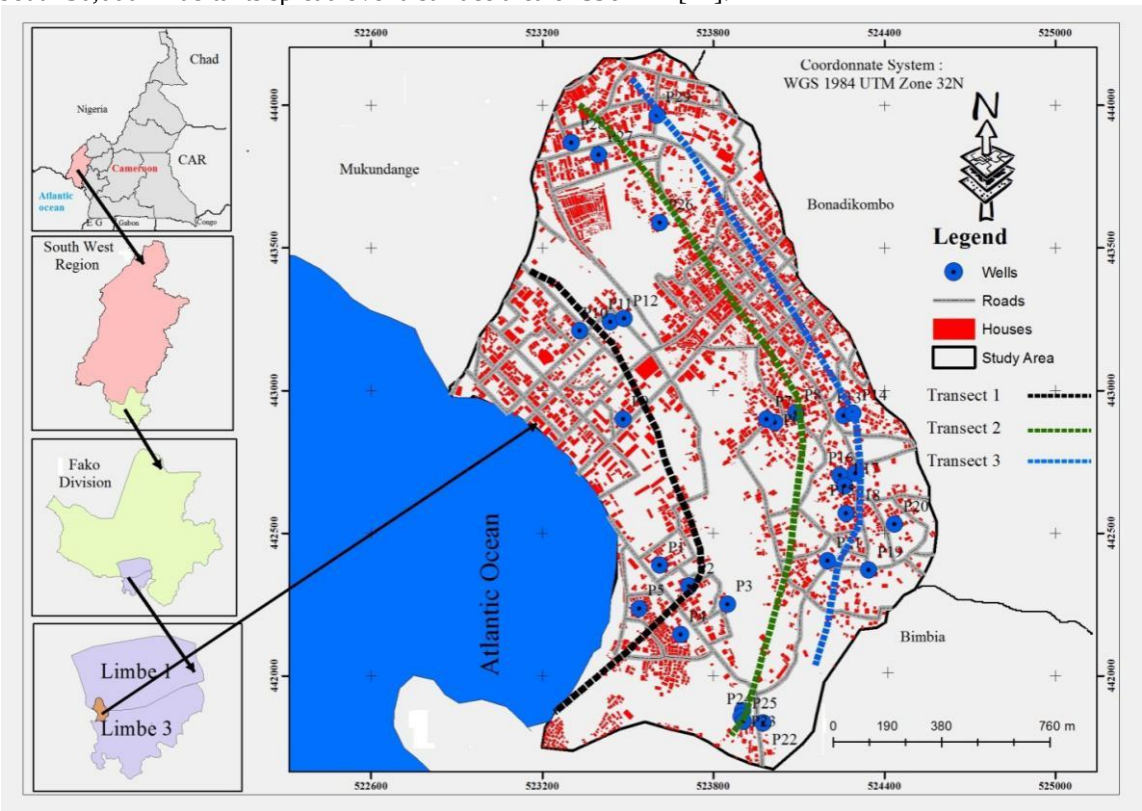

Figure 1. Location of the study area and location of sampling points in Limbe along three transects

The town is characterized by a low-lying coastal plain, rising up to a chain of horseshoe shaped hills towards the northeast and east, with the highest point at 362 m above sea level [23]. Within the town, small rivers flow into larger drainage channels that converge into the main river (Njenguele) that empties into the Atlantic Ocean (Figure 2). These rivers frequently overflow their banks in the rainy season causing floods in the low-lying areas that are only 1–2 m above sea level [24]. The hills that surround the town are made up of loose ferralitic and volcanic soils that easily disintegrate when the water content is high [25].

(This work is licensed under a Creative Commons Attribution 4.0 International License.)

International Journal of Engineering Research & Technology (IJERT)
ISSN: 2278-0181
Vol. 9 Issue 11, November-2020

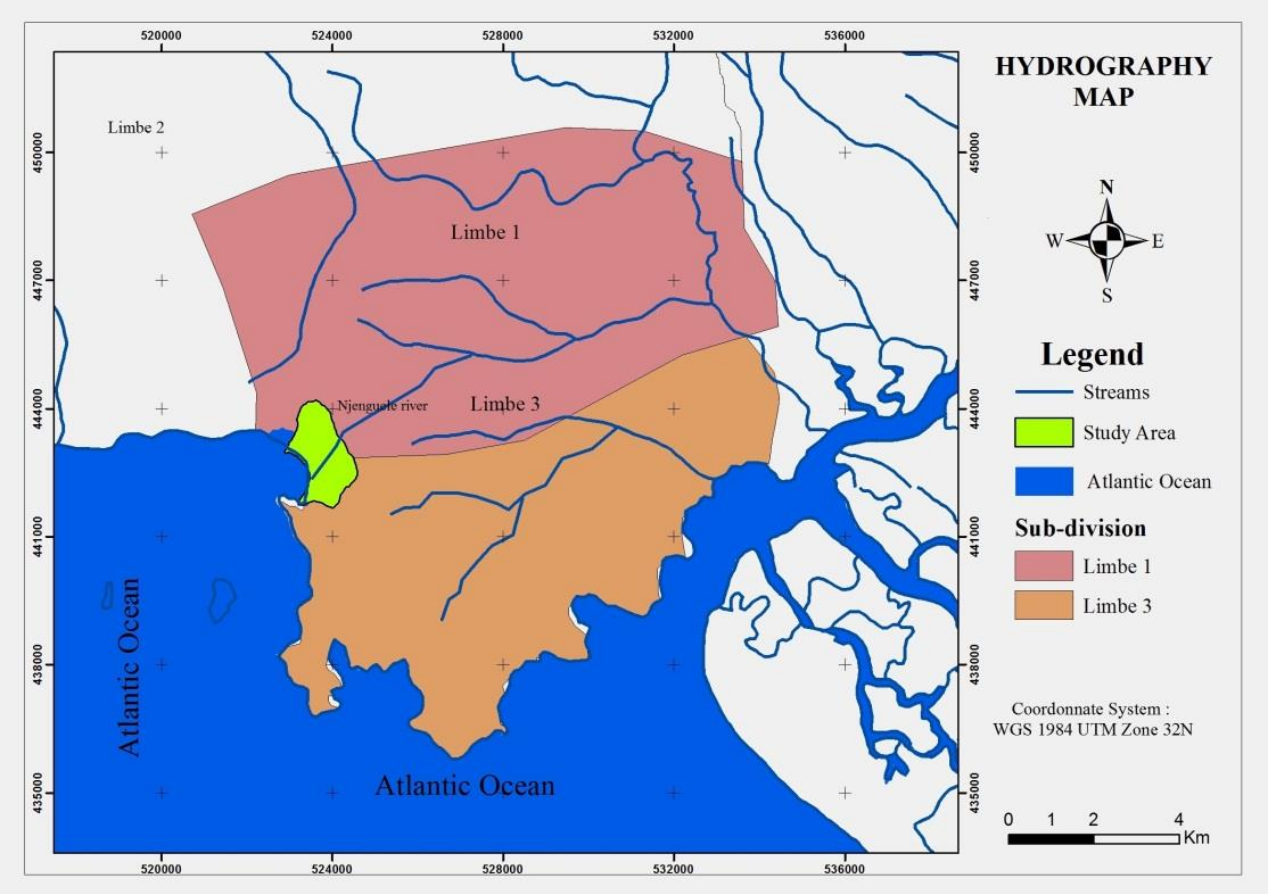

Figure 2. Hydrography of Limbe, a coastal town in Cameroon

Source: [26]

(ii) Climate

The climate of Limbe is the sub-equatorial type with two distinct seasons: a dry season of two months from December to January and a rainy season of 10 months from February to November with a mean annual rainfall of 3,100 mm, ±1,100 standard deviation [27]. The monthly rainfall frequently exceeds 500 mm and sometimes is over 1,000 mm in June, July and August. The mean annual temperature is about 26 °C while the relative humidity is generally above 85% [28].

(iii) Geomorphology and Hydrogeology

The study area is made up of ridges (Alpha club Hills, White man Hills, Caterpillard Hills, Mbende Hills, Towel Hills, Mile two Hills, Mabeta New layout Hills) and deeply incised ravines with a W–E orientation at a high angle to the general NE–SW orientation of Mount Cameroon [27]. These ridges form part of the Limbe-Mabeta Volcanic Massif, made up of degraded and deeply weathered tertiary basaltic lava flows [27]. The elevations in the study area range from 0 to about 90 m above sea level with slopes ranging from 0° to 43° (Figure 3). The main rock types within this area include basalts (Figure 4), basanites, lahar deposits, and pyroclastic materials [26].

The hydrogeology is characterized by unfossiliferous sandstone and gravel, weathered from underlying Precambrian basement rock [29]. It consists of Coastal Plain Sands (CPS) and recent sediments. The CPS aquifer is the most productive and exploited aquifer in Limbe.

(This work is licensed under a Creative Commons Attribution 4.0 International License.)

International Journal of Engineering Research & Technology (IJERT)
ISSN: 2278-0181
Vol. 9 Issue 11, November-2020

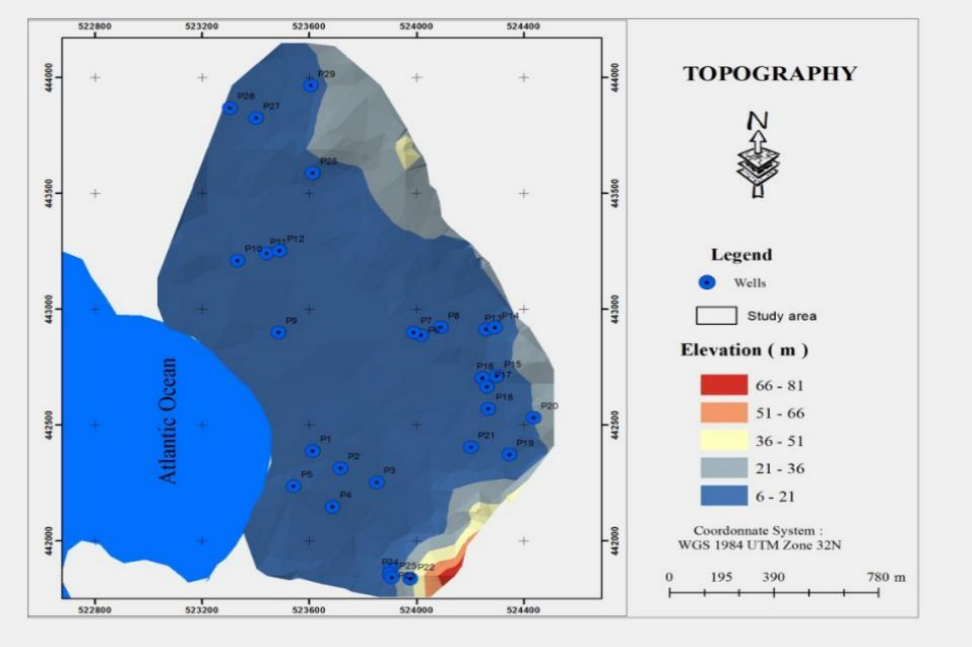

Figure 3. Topographic map of the study area

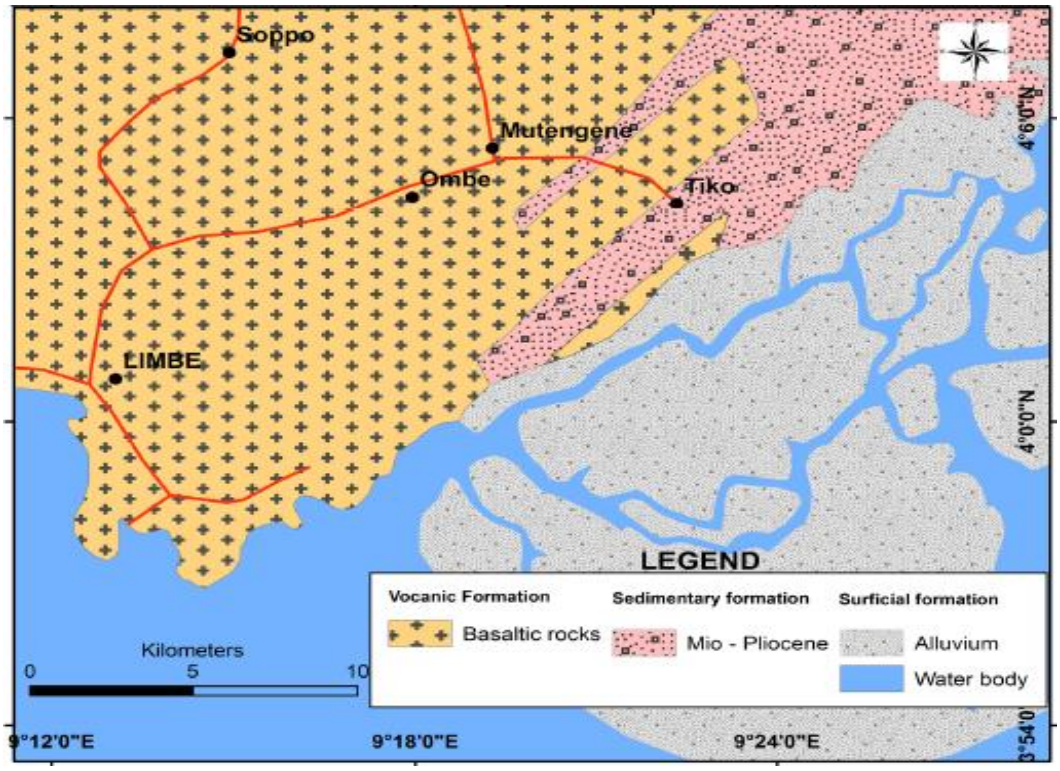

Figure 4. Geologic map of the study area

Source : [30]

B. Data collection and analysis

Water samples were collected monthly between July 2017 and June 2018 from thirty hand dug wells located along three transects as shown on Figure 1. The sample size was determined using the formulae presented in (1) and (2) [31]:

$$m = \frac{z^2}{\varepsilon^2} * p * (1 - p) \quad (1)$$

(This work is licensed under a Creative Commons Attribution 4.0 International License.)

International Journal of Engineering Research & Technology (IJERT)
ISSN: 2278-0181
Vol. 9 Issue 11, November-2020

$$n = \frac{m}{1+\frac{m-1}{N}} \quad (2)$$

Where:
m = the sample size.
n = the correction sample size for a limited population.
N = the population.
z = the value related with confidence level (1.96 for 95% confidence level).
p = the degree of variance between the elements of population (0.5).
ε = the maximum error (0.07).

The electrical conductivity (EC), the pH and the total dissolved solids (TDS) where measured in situ using a portable hand held, pH-028 six in one monitor. Water samples for laboratory analysis were collected in clean 150 ml polyethylene bottles and preserved in ice chests for analyses of chloride and bicarbonate using standard methods [32].

The co-ordinates of the sampled wells were recorded using a Global Positioning System (GPS) and there after were plotted using ArcGIS software on the geomorphological map of Limbe. To get a comprehensive picture of the overall quality of groundwater, the water quality index (WQI) was used. WQI is defined as a rating reflecting the composite influence of different water quality parameters on the overall quality of water. He [33] proposed the following (3) for calculating the Revelle Index (RI) which is used to assess groundwater pollution from seawater:

$$RI = \frac{[Cl^-]}{[HCO_3^-]+[CO_3^{2-}]} \quad (3)$$

Where:
$[Cl^-]$ = the concentration of chloride in the sample in mg/l
$[HCO_3^-]$ = the concentration of bicarbonate in the sample in mg/l
$[CO_3^{2-}]$ = the concentration of carbonate in the sample in mg/l

According to [33] when RI < 0.5, this indicates there is no sea water intrusion; when RI is between 0.5-6.6, this indicates the gw is slightly affected and when its greater than 6.6 it indicates its strongly affected.

The drinking water quality was assessed using a water quality index (WQI) and the [12] standard. The stages of calculating the WQI are as follows:

$$q_n = 100\frac{V_n - V_{io}}{S_n - V_n} \quad (4)$$

Where:
q_n = quality rating for the n^{th} water quality parameter
n = the water quality parameter and quality rating or sub index (q_n) corresponding to n^{th} parameter i.e. a number reflecting the relative value of this parameter with respect to its standard (maximum permissible value)
V_n = estimated value of the n^{th} parameter at a given the sampling point
S_n = standard permissible value of the n^{th} parameter
V_{io} = ideal value of n^{th} parameter in pure water i.e. 0 for all other parameters except pH and dissolved oxygen (7.0 and 14.6 mg/l respectively).

The unit weight of the n^{th} parameter (W_n) was calculated by a value inversely proportional to the recommended standard value (S_n) of the corresponding parameter.

$$W_n = \frac{K}{S_n} \quad (5)$$

Where:
S_n = standard value for the n^{th} parameters
K = proportionality constant ($K = \frac{1}{\Sigma(\frac{1}{S_n})}$)

The WQI was then calculated using (6):

$$WQI = \frac{\Sigma q_n w_n}{\Sigma w_n} \quad (6)$$

Table 1 shows the classification of water based on the WQI from the point of potability.

Table 1. Water quality index and status of water quality

Water Quality Index	Water Quality Class
0-25	Excellent water quality
26-50	Good water quality
51-75	Poor water quality
76-100	Very poor water quality
Above 100	Unsuitable for drinking

Source: [34]

The coordinates of each sample were determined using a Garmin GPSmap 78S. The values of the Revelle Index and the Water Quality Index were then exported to the ArcGIS 6.0 software and used to generate maps of their spatial distribution over

(This work is licensed under a Creative Commons Attribution 4.0 International License.)

International Journal of Engineering Research & Technology (IJERT)
ISSN: 2278-0181
Vol. 9 Issue 11, November-2020

the study area. The areas referring to each water quality class and the Revelle Index were circumscribed on the map using ArcGIS6.0. They were automatically generated with this software surface function. Finally, slicing options were applied using these ranges of values with five groups of water quality classes to generate a spatial distribution of water quality map [34]. The statistical analysis of the examined groundwater parameters was computed using STATA software version 6.0.

C. Effect of CC on sea water intrusion

The effect of CC on sea water intrusion in the study area was determined using the estimation of the SLR; the determination of the retreat in the shoreline; the hydraulic head of the coastal aquifer due to CC and the velocity of the gw. Reference [6] showed that there was a correlation between sea level and the temperature of ocean surface waters at Limbe in Cameroon. This study noted the increase in sea level at the Limbe coasts of 10 mm / year and a retreat in the shoreline of 32 cm / year. This recession will leave a space favorable to saline intrusion, the consequence of which will be the advancement of the salt water front. The projection of the sea level rise for 2050 and 2100 were obtained by using the (7) and (8) respectively.

$$SLR_{2050} = \text{annual rate of SLR x } (2050 - 2018) \quad (7)$$

$$SLR_{2100} = \text{annual rate of SLR x } (2100 - 2018) \quad (8)$$

The projected retreat or recession in the shoreline in 2050 and 2100 were obtained using (9) and (10) respectively.

$$\text{Retreat in the shoreline in 2050} = \text{annual retreat in the shoreline rate x } (2050 - 2018) \quad (9)$$

$$\text{Retreat in the shoreline in 2100} = \text{annual retreat in the shoreline rate x } (2100 - 2018) \quad (10)$$

The velocity of flow of the gw in 2018 was obtained using Darcy's formula in (11):

$$v = Ki \quad (11)$$

where:

v = velocity of flow of the gw (cm/s)
K = soil permeability (cm/s)
i = hydraulic gradient (ratio)

The soil permeability was obtained using the Porchet method (Figure 6). For this, a cylindrical hole was dug with an auger 10 cm in diameter and 50 cm deep. After filling the hole with water, the height of the water h_1 was noted at time t_1 and later h_2 at time t_2.

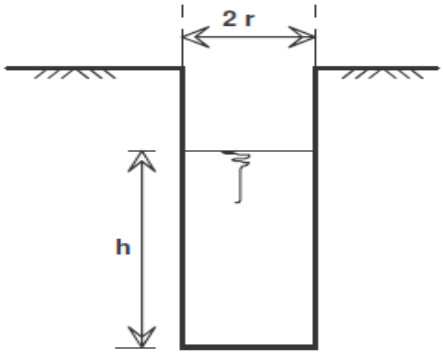

Figure 6. Measurement of the infiltration rate by the Porchet method

Source: [35]

The permeability of the soil K was obtained from (12).

$$K = \frac{r}{2(t_2 - t_1)} \ln \frac{(h_1 + \frac{r}{2})}{(h_2 + \frac{r}{2})} \quad (12)$$

where:

K = soil permeability (cm/s)
r = radius of the hole (cm)
h_1 = height of the water (cm) at time t_1 (s)
h_2 = height of the water (cm) at time t_2 (s)

In a free porous type aquifer, the dominant flows are horizontal, consequences of a weak hydraulic gradient in low lying areas [36]. The piezometric level is influenced by the geometry, the topography, the hydrodynamic properties of the soil and the operating conditions. From the base year of 2018; wells that had been affected by salt intrusion were retained because their hydraulic heads were greater than the other wells. The salty well (P_3) with the highest hydraulic head and the well (P_9) with the lowest hydraulic head were used for the estimation of the hydraulic gradient.

The hydraulic gradient of the aquifer water was determined using (13):

(This work is licensed under a Creative Commons Attribution 4.0 International License.)

International Journal of Engineering Research & Technology (IJERT)
ISSN: 2278-0181
Vol. 9 Issue 11, November-2020

$$i = \frac{dh}{dl} \quad (13)$$

where:

i = hydraulic gradient (ratio)

dh = the difference in head compared to an upstream well and a downstream well (m).

dl = the distance between the two wells (m).

The salt front was measured from the coastline with the "distance measurement" application in ArcGIS software. As the sea level rose, this front had to move from the highest hydraulic head to the lowest due to the increased hydraulic head in the wells in the critical zone. The simulation of [36] gives the hydraulic head in the coastal aquifer equal to half the rise in sea level during this period and this was used in the study. The salt front during displacement affected new wells (P_6, P_7, P_{10}) with concentrations equal to those of wells from the initial position of the salt front. These new concentrations were substituted with the old concentrations from where the Revelle indices for 2050 and 2100 (only well P_8 was affected and P10 excluded) were calculated according to the formulas of (14) and (15):

$$RI_{2050} = \frac{[Cl^-]_{2050}}{[HCO_3^-]+[CO_3^{2-}]} \quad (14)$$

$$RI_{2100} = \frac{[Cl^-]_{2100}}{[HCO_3^-]+[CO_3^{2-}]} \quad (15)$$

For the projections with rising sea levels due to climate change, the hydraulic gradients for the years 2050 and 2100 were estimated based on the (16) and (17) The new velocity of the salt fronts for these respective years were obtained with the (18) and (19) and finally the projected displacement of the salty front were obtained with (20) and (21) respectively for 2050 and 2100

$$i_{2050} = \frac{dh_{2050}}{dl} \quad (16)$$

$$i_{2100} = \frac{dh_{2100}}{dl} \quad (17)$$

$$v_{2050} = Ki_{2050} \quad (18)$$

$$v_{2100} = Ki_{2100} \quad (19)$$

$$d_{2050} = v_{2050}t_{50} \quad (20)$$

$$d_{2100} = v_{2100}t_{100} \quad (21)$$

where:

i_{2050} and i_{2100} are the hydraulic gradients in 2050 and 2100 respectively

dh_{2050} and dh_{2100} are the difference in load compared to an upstream well and a downstream well in 2050 and 2100 respectively (m)

dl = the distance between the two wells (m)

v_{2050} and v_{2100} are the velocities of gw in 2050 and 2100 respectively (cm/s)

K is the soil permeability (cm/s)

d_{2050} and d_{2100} are displacements of the salt front in 2050 and 2100 respectively (m)

t_{50} = 2050-2018 =32 years

t_{100} = 2100-2050 = 50 years

As the hydraulic gradient will change with the sea level, the impact will be on the concentration of chloride. WQI for the years 2050 and 2100 were obtained with (22) and (23) respectively.

$$WQI_{2050} = \frac{q_{pH} * W_{pH} + q_{TDS} * W_{TDS} + q_{EC} * W_{EC} + q_{[Cl^-]_{2050}} * W_{[Cl^-]_{2050}} + q_{[HCO_3^-]} * W_{[HCO_3^-]}}{W_{pH} + W_{TDS} + W_{EC} + W_{[Cl^-]_{2050}} + W_{[HCO_3^-]}} \quad (22)$$

$$WQI_{2100} = \frac{(q_{pH} * W_{pH}) + (q_{TDS} * W_{TDS}) + (q_{EC} * W_{EC}) + (q_{[Cl^-]_{2100}} * W_{[Cl^-]_{2100}}) + (q_{[HCO_3^-]} * W_{[HCO_3^-]})}{W_{pH} + W_{TDS} + W_{EC} + W_{[Cl^-]_{2100}} + W_{[HCO_3^-]}} \quad (23)$$

(This work is licensed under a Creative Commons Attribution 4.0 International License.)

International Journal of Engineering Research & Technology (IJERT)
ISSN: 2278-0181
Vol. 9 Issue 11, November-2020

where

q_{pH} = quality rating for the pH
q_{TDS} = quality rating for the TSD
q_{EC} = quality rating for the CE
$q_{[Cl^-]_{2050}}$ = quality rating for the chloride in 2050
$q_{[HCO_3^-]}$ = quality rating for the bicarbonate
$q_{[Cl^-]_{2100}}$ = quality rating for the chloride in 2100

W_{pH} = unit weight for the pH

W_{TDS} = unit weight for the TDS

W_{EC} = unit weight for the EC

$W_{[Cl^-]_{2050}}$ = unit weight for the chloride in 2050

$W_{[Cl^-]_{2100}}$ = unit weight for the chloride in 2100

$W_{[HCO_3^-]}$ = unit weight for the bicarbonate

WQI_{2050} and WQI_{2100} were imported to the software ArcGIS for digitizing maps. The areas occupied by the various water quality classes were obtained after circumscribing each color with the "surface" application of the software.

III. RESULTS AND DISCUSSION

A. Effect of CC on sea water intrusion in Limbe

Following the correlation between sea level and the temperature of ocean surface waters in Limbe, the rise was estimated to be of 10 mm/ year and a receeding shoreline of 32 cm/ year in 2018. In 2050 the rise in sea level was estimated to be 32 cm compared to the reference year of 2018, while the coastline receeded by 1.024 m. In 2100, the rise in sea level was determined to be 82 cm and will lead to the coast line receeding by 2.624 m compared to the 2018 value.

The salt front was determined with ArcGIS to be located at 779 m from the coastline in 2018. The hydraulic gradient was negative with a value of -0.405% in the area occupied by wells P_1, P_2, P_3, P_4, P_5 and P_9 as shown in Figure 7. This gradient was given with wells P_3 and P_9. The velocity of the gw in this critical area was 9.35 mm/day with an average permeability in the study area initially found of 2.308 m/day in 2018. It is projected that the velocities of the aquifer subsequent to sea level rise will be 9.75 mm/day and 10.60 mm/day respectively in 2050 and 2100. The salt fronts will be about 114 m in 2050 compared to the position in 2018, and 317 m in 2100 compared to 2050. Studies had revealed that the rate of recession of the coast line in Rio Del Rey in the Bakassi peninsula in Cameroon was 10 m/year [37]. This is much higher than the rate of 32cm/year determined in this study. It is also very different from the values found on the Togolese and Beninese coasts where the coastal drift is more pronounced on the coasts. Reference [38] found that the rate of recession of the coastline in Benin was about 12 m/year on a segment of coast of approximately 5 km for more than ten years. In Togo, the consequence has been the relocation of the Accra-Cotonou motoway twice; loss of land and displacement of local populations living exclusively on fishing. Elsewhere, even if the available data are less alarming, they are no less worrying. In Ivory Coast for example, the recession of the coastline vary on average from one to three meters per year [39].

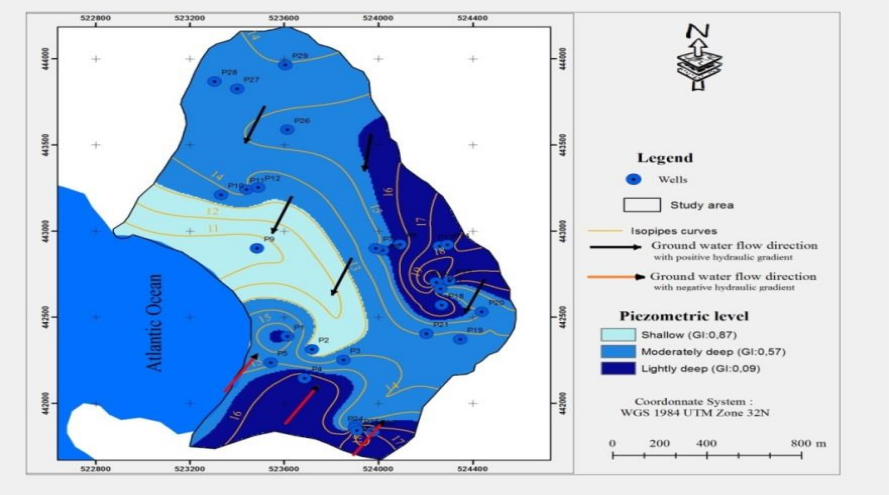

Figure 7. Piezometric map of the study area

(This work is licensed under a Creative Commons Attribution 4.0 International License.)

International Journal of Engineering Research & Technology (IJERT)
ISSN: 2278-0181
Vol. 9 Issue 11, November-2020

B. Extent of sea water intrusion in the coastal aquifer in a changing a climate

In the study area, RI varied from 0.126 to 1.551 as shown in Table 2. According to Revelle (1941) [33], this suggests that some areas in the study area have not been affected (RI less than 0.5) while others have been slightly affected (RI is between 0.5 and 6.6). The relationship between the ratios of $\frac{[Cl^-]}{[HCO_3^-]+[CO_3^{2-}]}$ indicates a strong positive linear relation with Cl^- concentrations (r = 0.94, p < 0.01).This linear relationship indicates the mixing of saline water and fresh groundwater [15]. Figure 8 shows the extent of the groundwater salinization in the study area. From Table 3, about 77% of the groundwater in the study area was unaffected by sea water intrusion, while 23% of the aquifer was slightly affected by pollution from sea water in 2018. The hotspots include locations of wells P_1, P_2, P_3, P_4, and P_5. Thus, efforts should be made to reduce the pollution of ground water due to sea level rise in the area.

Table 2. Revelle Index of gw in the study area

Transects	Wells	Coordinates (meters)		Revelle index		
		X	***Y***	***2018***	***2050***	***2100***
T1	P1	523612	442388	1.089	1.089	1.089
T1	P2	523716	442314	1.356	1.356	1.356
T1	P3	523850	442252	1.018	1.018	1.018
T1	P4	523686	442146	1.249	1.249	1.249
T1	P5	523541	442236	1.551	1.551	1.551
T1	P9	523484	442900	1.061	1.061	1.061
T1	P10	523331	443210	0.41	0.71	0.41
T1	P11	523439	443241	0.436	0.436	0.436
T2	P6	524016	442888	0.424	0.746	0.746
T2	P7	523988	442900	0.393	0.57	0.57
T2	P8	524090	442922	0.461	0.461	0.661
T2	P12	523488	443253	0.328	0.489	0.489
T2	P15	524299	442711	0.184	0.184	0.184
T2	P16	524245	442703	0.287	0.287	0.287
T2	P17	524262	442665	0.317	0.317	0.317
T2	P18	524267	442570	0.356	0.356	0.356
T2	P19	524346	442372	0.201	0.201	0.201
T2	P21	524202	442404	0.357	0.357	0.357
T2	P26	523612	443589	0.549	0.549	0.549
T2	P27	523399	443827	0.485	0.485	0.485
T2	P28	523303	443870	0.383	0.383	0.383
T2	P29	523604	443966	0.398	0.398	0.398
T2	P30	523634	443866	0.313	0.313	0.313
T3	P13	524259	442912	0.244	0.244	0.244
T3	P14	524291	442921	0.461	0.461	0.461
T3	P20	524437	442532	0.322	0.322	0.322
T3	P22	523976	441835	0.126	0.126	0.126
T3	P23	523903	441878	0.14	0.14	0.14
T3	P24	523899	441857	0.131	0.131	0.131
T3	P25	523907	441841	0.132	0.132	0.132
			Min	0.126	0.126	0.126
			Max	1.551	1.551	1.551
			Mean	0.505	0.537	0.534
			Std	0.389	0.390	0.389

(This work is licensed under a Creative Commons Attribution 4.0 International License.)

International Journal of Engineering Research & Technology (IJERT)
ISSN: 2278-0181
Vol. 9 Issue 11, November-2020

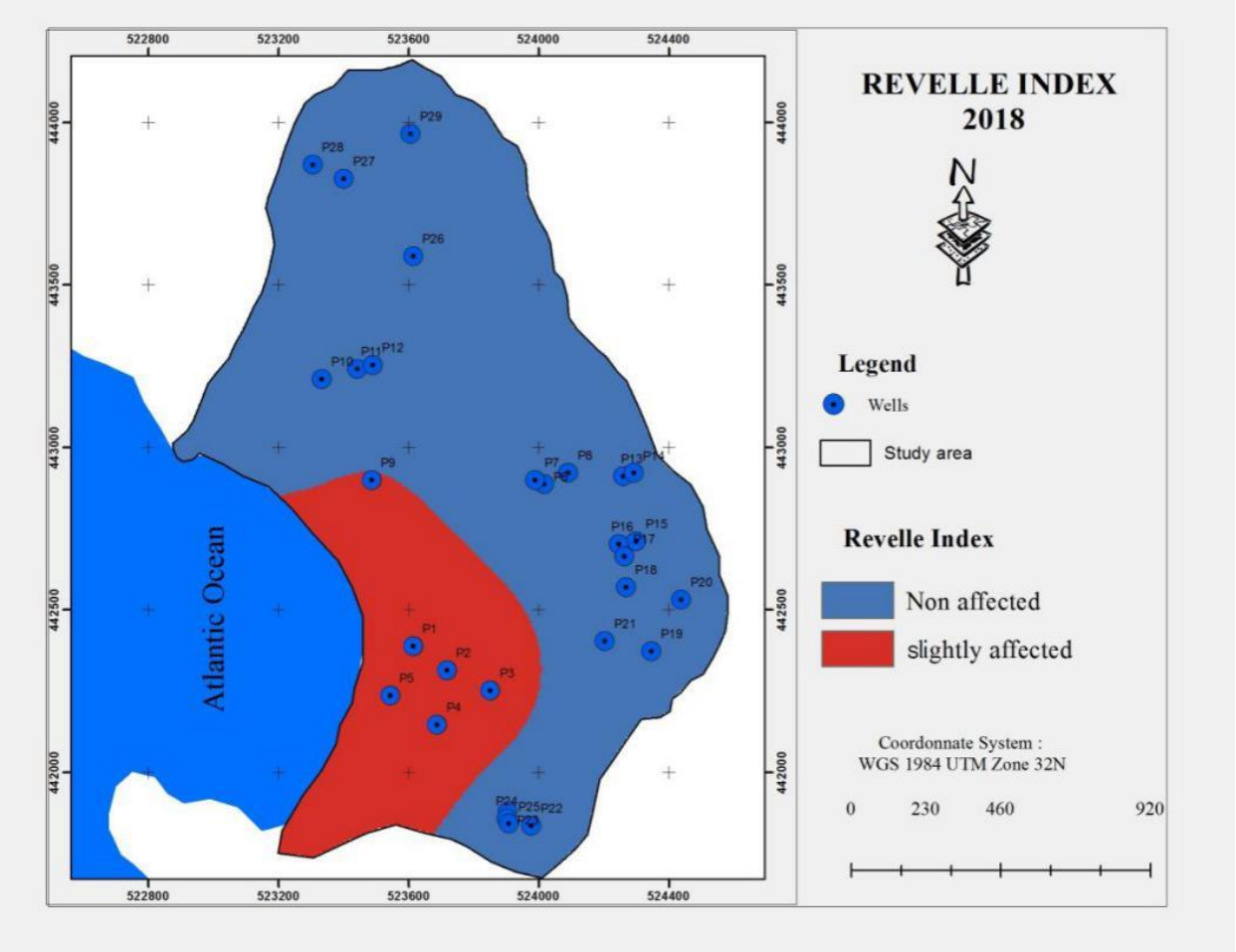

Figure 8. Spatial variation of sea water intrusion into ground water in Limbe in 2018

With the projected sea level rise (SLR) of 32 cm in 2050 and 82 cm in 2100 due to climate change from the 2018 the base year, the hydraulic head will be increased in the critical wells by 0.16 m in 2050 by of 0.492 m in 2100 based on simulations by [36]. A negative hydraulic gradient will be noted and will lead to the change in the RI. Figures 9 and 10 are show the spatial variations of sea water intrusion into ground water in 2050 and 2100 respectively as influenced by projected seal level rise. The area covered by various RI were calculated from the RI maps and given in Table 3. The area slightly affected will increase from 55.36 ha in 2018 to 74.32 ha in 2050 leading to an increment of 7.8 % of the total area lightly affected. The increment will be 11.51 % by the year 2100.

(This work is licensed under a Creative Commons Attribution 4.0 International License.)

International Journal of Engineering Research & Technology (IJERT)
ISSN: 2278-0181
Vol. 9 Issue 11, November-2020

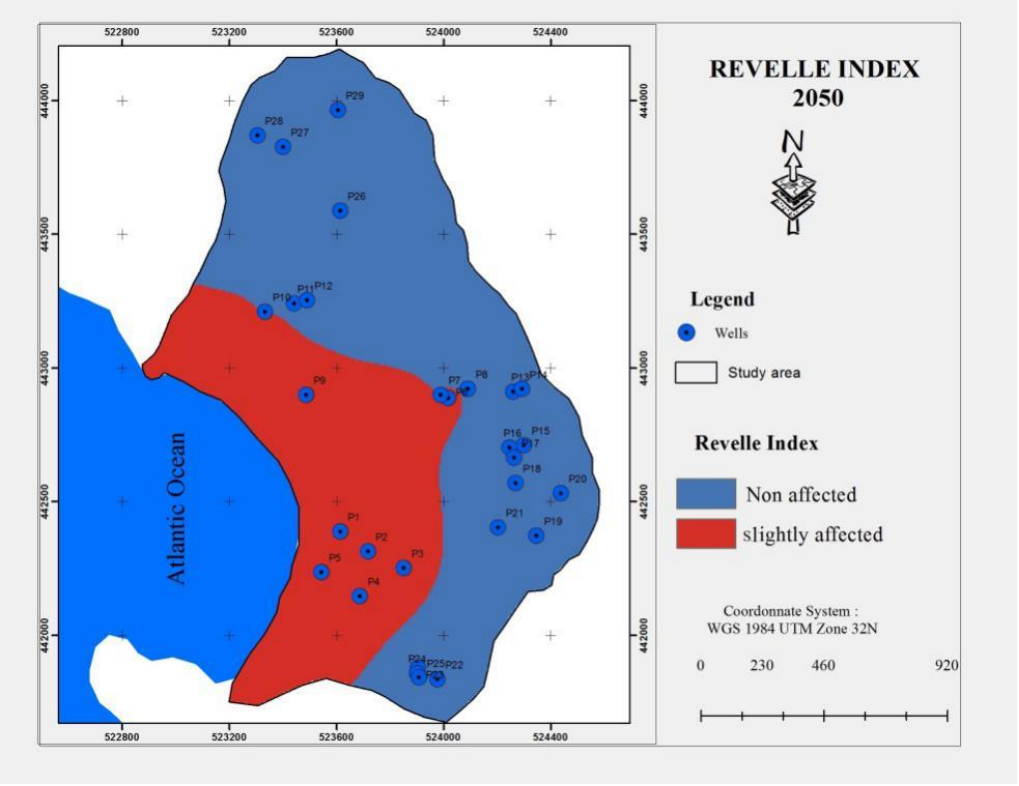

Figure 9. Projected spatial variation of sea water intrusion into ground water in Limbe in 2050

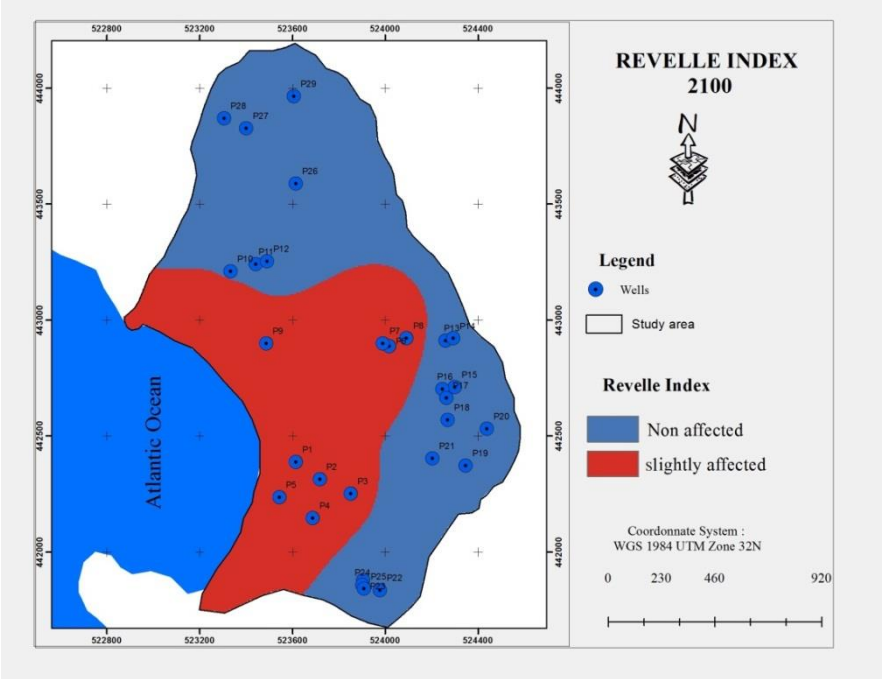

Figure 10. Projected spatial variation of sea water intrusion into ground water in Limbe in 2100

Table 3. Extent of sea water intrusion into ground water in Limbe

Degree of sea water intrusion	**2018**		**2050**		**2100**	
	Area, (ha)	***Percentage of total***	***Area, (ha)***	***Percentage of total***	***Area, (ha)***	***Percentage of total***
Non affected	185.96	77	167	69.20	139.21	57.69
Slightly affected	55.36	23	74.32	30.8	102.11	42.31
Total	241.32	100	241.32	100	241.32	100

(This work is licensed under a Creative Commons Attribution 4.0 International License.)

International Journal of Engineering Research & Technology (IJERT)
ISSN: 2278-0181
Vol. 9 Issue 11, November-2020

C. Extent of the gw suitable for drinking

The suitability of groundwater for drinking purposes in the study area was determined using WHO (2006) [12] guidelines. The computed WQI ranged from 28 to 115 as indicated in Table 4.

Table 4. Water quality index in the study area

Transects	Wells	Coordinates (m)		WQI		
		X	*Y*	*2018*	*2050*	*2100*
T1	P1	523612	442388	84	84	84
T1	P2	523716	442314	108	108	108
T1	P3	523850	442252	93	93	93
T1	P4	523686	442146	115	115	115
T1	P5	523541	442236	114	114	114
T1	P9	523484	442900	73	73	73
T1	P10	523331	443210	67	67	67
T1	P11	523439	443241	84	84	84
T2	P6	524016	442888	72	77	77
T2	P7	523988	442900	96	102	102
T2	P8	524090	442922	97	100	100
T2	P12	523488	443253	69	86	86
T2	P15	524299	442711	28	28	49
T2	P16	524245	442703	29	29	40
T2	P17	524262	442665	35	35	44
T2	P18	524267	442570	57	57	57
T2	P19	524346	442372	28	28	28
T2	P21	524202	442404	42	42	42
T2	P26	523612	443589	44	44	44
T2	P27	523399	443827	64	64	64
T2	P28	523303	443870	53	53	53
T2	P29	523604	443966	42	42	42
T2	P30	523634	443866	48	48	48
T3	P13	524259	442912	51	51	51
T3	P14	524291	442921	48	48	48
T3	P20	524437	442532	41	41	41
T3	P22	523976	441835	40	40	40
T3	P23	523903	441878	40	40	40
T3	P24	523899	441857	44	44	44
T3	P25	523907	441841	43	43	43
			Min	**28**	**28**	**28**
			Max	**115**	**115**	**115**
			Mean	**62**	**63**	**64**
			Standard deviation	**26.41**	**27.27**	**25.91**

The area covered by different water quality classes were calculated from the WQI maps (Figure 11, 12 and 13 respectively for 2018, 2050 and 2100) and are presented in Table 5. About 34.4 % of the gw is currently considered to be good for drinking while 65.6 % is either poor, very poor or unsuitable for drinking. As the years go by, based on projected sea level rise due to climate change, the amount of sea water intrusion is set to increase if there are no mitigating measures. The proportion of gw considered to be of good quality is therefore projected to reduce as more gw becomes polluted by sea water. From Table 5, in 2050, the proportion of the ground water considered to be good for drinking will reduce to 26.92 % and down to 17.86 % in 2010. Hot spots that require attention are wells P_2, P_3, P_4 and P_5, all along transect 1, which is closest to the sea. The EC, pH, TDS, Cl^- and HCO_3^- all contributed to the WQI values. However, values of chloride and electrical conductivity were the main parameters responsible for the high values of WQI. In some locations, the TDS also significantly increased the WQI.

(This work is licensed under a Creative Commons Attribution 4.0 International License.)

International Journal of Engineering Research & Technology (IJERT)
ISSN: 2278-0181
Vol. 9 Issue 11, November-2020

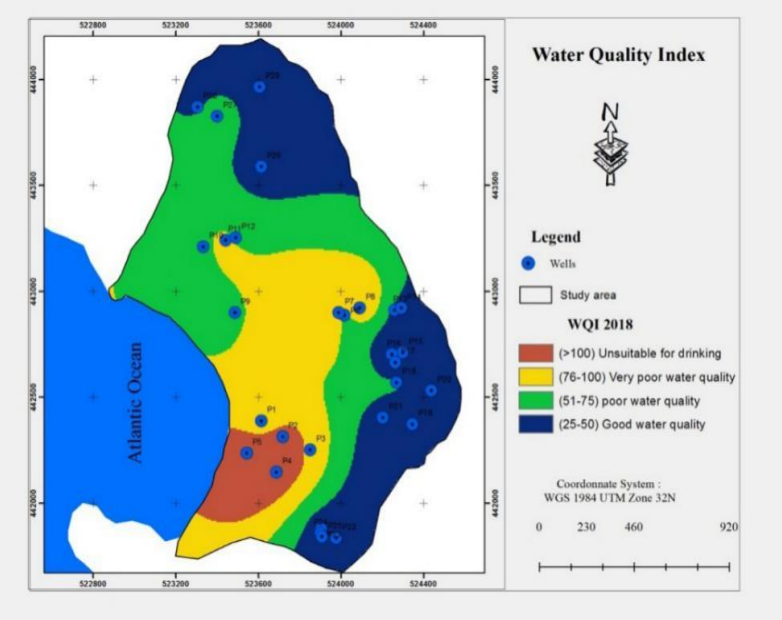

Figure 11. Spatial variation of ground water quality in Limbe in 2018

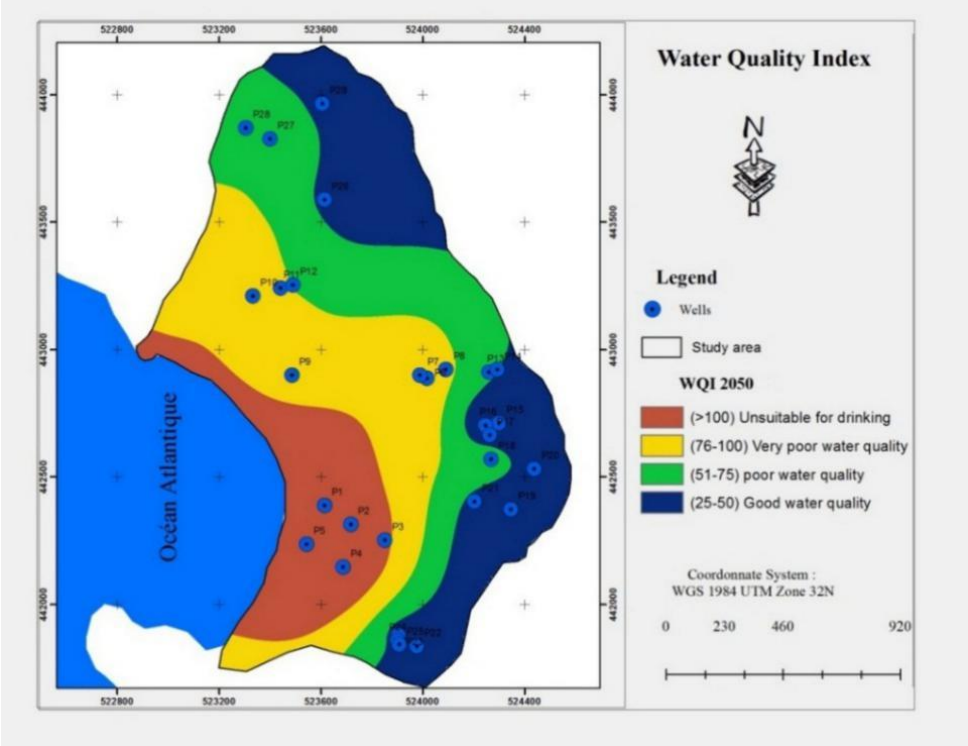

Figure 12. Spatial variation of ground water quality in Limbe in 2050 (sea level rises 0.32 m)

(This work is licensed under a Creative Commons Attribution 4.0 International License.)

International Journal of Engineering Research & Technology (IJERT)
ISSN: 2278-0181
Vol. 9 Issue 11, November-2020

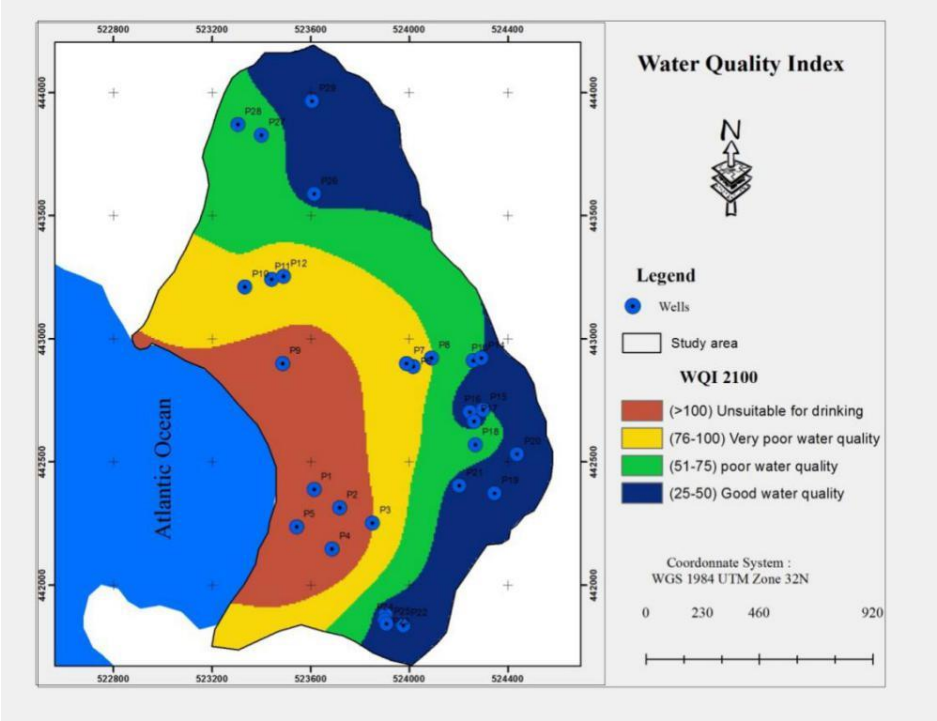

Figure 13. Spatial variation of ground water quality in Limbe in 2100 (sea level rises 0.82 m)

Table 5. Proportion of different water quality classes in the study area.

Water quality class	2018		2050		2100	
	(ha)	***Percentage of total***	***(ha)***	***Percentage of total***	***(ha)***	***Percentage of total***
Unsuitable for drinking	16.38	6.79	42.78	17.73	60.65	25.13
Very poor	60.63	25.12	70.68	29.29	68.55	28.41
Poor	81.30	33.69	62.90	26.06	69.02	28.60
Good	83.01	34.40	64.96	26.92	43.10	17.86
Total	241.32	100	241.32	100	241.32	100

D. Measures to reduce sea water intrusion

About 23% of the aquifer of the study area is affected by sea water intrusion rendering the water non-potable. In order to reduce the intrusion of ocean water, there are two possibilities; construction of dykes or barriers; and planting a halophyte plant. Anti-salt barriers or dykes can be used to combat saline intrusion [40]. However, they are limited in that they are effective only in controlling surface sea water flow but, they do not prevent the intrusion of underground sea water [41].

A more effective solution is the planting of halophyte plants like mangrove trees of the Rhizophoraceae family. They should be planted on both sides of the mouth of the River Njenguele over a distance of 500 m. Mangrove trees stabilize the coastline and serve as a barrier against erosion due to swell by reducing the energy of the waves and by modifying the hydrocirculations [42]. Mangrove trees have a root system that filters water, and can thus exclude up to 90% of salts from interstitial waters thanks to glands located in their leaves [43]. Mangrove trees planted a short distance offshore, control high energy waves which erode the coastline and prevent the meeting of coastal marine waters and fresh waters. In addition, the complex geochemical reactions taking place in the sediment around the trees can immobilize toxic metals and consequently purify coastal waters. Furthermore, mangrove trees serve as a natural barrier against the gradual rise in mean sea level and saline intrusion into aquifers and arable land. They also have a significant refuge value and hence they enhance aquatic biodiversity.

IV. CONCLUSIONS

Based on the methodology used in this study and the results obtained, it can be concluded that:

(1) The sea level rise is projected to rise in Limbe by 32 cm in 2050 and 82 cm in 2100 (from the base year of 2018) due to climate change.

(2) About 23% of the ground water in study area is presently slightly polluted by seawater intrusion. By 2050, this is projected to increase to 30.8 % and to 42.31 % in 2100 due increased sea water intrusion resulting from sea level rise because of climate change.

(3) About 34.4 % of the ground water in the study area is currently considered to be good for drinking while 65.6 % is either poor, very poor or unsuitable for drinking. By 2050, the proportion of the ground water considered to be good for drinking

(This work is licensed under a Creative Commons Attribution 4.0 International License.)

International Journal of Engineering Research & Technology (IJERT)
ISSN: 2278-0181
Vol. 9 Issue 11, November-2020

in Limbe will reduce to 26.92 % and down to 17.86 % in 2100. Hot spots that require urgent attention are locations of wells P_2, P_3, P_4 and P_5

(4) To minimize the impact of sea water intrusion on the quality of gw in the study area a halophyte plant like mangrove should be planted at the mouth of River Njenguele, which is the main natural drain in the study area.

DISCLOSURE STATEMENT

No potential conflict of interest was reported by the authors.

ACKNOWLEDGEMENTS

The authors are most grateful to the water utility company in Limbe for their collaboration in this study. Special thanks to all those who participated in the collection of data, in the laboratory analyses and to the population of the study area for their support.

REFERENCES

[1] P.G. Rejith, S.P. Jeeva, H. Vijith, M. Sowmya, and A.A.H Mohamed, "Determination of groundwater quality index of a highland village of Kerala (India) using geographical information system", *Journal of Environmental Health*, **71**, pp 51–58, **(2009)**.

[2] B.C. Douglas, "Global sea level rise: A redetermination. *Surveys in geophysics*", **18**, pp 279–292. **(1997)**.

[3] B. Bates, Z.W. Kundzewicz, S. Wu, J. Palutikof "Climate change and water. Technical Paper of the Intergovernmental Panel on Climate Change". Geneva, Switzerland: IPCC Secretariat, **(2008)**.

[4] Intergovernmental Panel on Climate Change (IPCC), "Climate change 2007," Cambridge, UK: Cambridge University Press, **(2007).**

[5] R.J. Nicholls and A. Cazenave, "Sea-level rise and its impacts on coastal zones," *Science*, **328**, pp 1517–1520, **(2010)**.

[6] R. Motchemien, "Effets de la variabilité du niveau de l'Océan Atlantique sur l'inondation continentale en zone urbaine à Limbé – Cameroun," Unpblished M.Sc thesis, University of Dschang, Dschang, Cameroon, **(2015)**.

[7] A.G. Werner and C.T. Simmons, "Impact of sea level rise on sea water intrusion in coastal aquifers," *Ground Water Journal*, **47**, 197-204, **(2009).**

[8] P.J. Lacombe and G.B, "Carleton Salt water intrusion into fresh ground-water supplies, southern Cape May County. Proceedings of the national symposium on the future availability of ground water resources, April 12-15, 1992 (pp 287-298), New Jersey, USA: USGS, **(1992)**.

[9] H.L. Li and J.J. Jiao, "Tide-induced seawater-groundwater circulation in a multi-layered coastal leaky aquifer system", *Journal of Hydrology*, **274**, pp 211-224, **(2003).**

[10] T. Feseker, "Numerical studies on salt water intrusion in a coastal aquifer in north western Germany", *Hydrogeology Journal*, **15**, pp 267–279, **(2007).**

[11] M.V. Esteller, R. Rodríguez, A. Cardona and L. Padilla-Sánche, "Evaluation of hydrochemical changes due to intensive aquifer exploitation: case studies from Mexico", *Journal of Environmental Monitoring and Assessment*, 9, pp 5725–5741 **(2012)**.

[12] World Health Organization (WHO), "Guidelines for drinking water quality," Geneva, Switzerland: WHO, **(2006)**.

[13] A. Sargaonkar and V. Deshpande, "Development of an overall index of pollution for surface water based on a general classification scheme in Indian context," *Journal of Environmental Monitoring and Assessment*, **89**, 43–67, **(2003)**.

[14] M.C. Shah, P.G. Shilpkar and P.B. Acharya, "Groundwater quality of Gandhinagar Taluka, Gujarat, India," *E-Journal of Chemistry*, **5**, pp 435–446, **(2008)**.

[15] A.A. Zaharin, M.H. Abdullah and S.M. Praveena, "Evolution of groundwater chemistry in the shallow aquifer of a small tropical island in Sabah. Malaysia," *Sains Malaysiana* 38(**6**).pp 805-812, **(2009)**.

[16] A.G. Chachadi and J.P. Lobo-Ferreira, "Sea water intrusion vulnerability mapping of aquifers using GALDIT method", In: Proc. Workshop on Modelling in Hydro-geology at Anna University (pp 143-156), Chennai, India: Anna University, **(2001)**.

[17] I.S. Akoteyon, "Evaluation of groundwater quality using water quality indices in parts of Lagos-Nigeria," *Journal of Environmental Geography*, **6**, 29-36, **(2013)**.

[18] M. Vasanthavigar, K. Srinivasamoorthy, K. Vijayaragavan, R. Ganthi, S. Chidambaram, P. Anandhan, R. Manivannan and S. Vasudevan, "Application of water quality index for groundwater quality assessment: Thirumanimuttar Sub-basin, Tamilnadu India," *Journal of Environmental Monitoring and Assessment*, **171**, pp 595–609, **(2010)**.

[19] C.R. Ramakrishnaiah, C. Sadashivaiah and G. Ranganna, "Assessment of water quality index for the groundwater in Tumkur Taluk, Karnataka State, India," *E-Journal of Chemistry*, **6**, pp 523–530, **(2009)**.

[20] S.G. Rao and G. Nageswararao, "Assessment of groundwater quality using water quality index," *Archives of Environmental Science*, **7**, pp 1-5, **(2013).**

[21] P. Sahu and P.K. Sikdar, "Use of water quality indices to verify the impact of Cordoba city (Argentina) on Suquy´a River," *Geology journal*, **55**, pp 823–835, **(2008)**.

[22] Institut National de Statistiques (INS), "Annuaire statistique du Cameroun," Yaoundé, Cameroun: INS, **(2013)**.

[23] R.K. Njabe, R. Fobang, "Illustrated physical geography and map reading for Cameroon," 3rd ed. Limbe, Cameroon: Sunway, **(2006)**.

[24] R. Ndille and J.A. Belle, "Managing the Limbe floods: Considerations for disaster risk reduction in Cameroon," *International Journal of Disaster Risk Science*, **5**, pp 147–156, **(2014)**.

[25] O.C. Nwankiti, "Man and his environment," London, UK: Longman Group, **(1983)**.

[26] W.G. Buh, "Geographic information systems-based demarcation of risk zones: the case of the Limbe Sub-Division – Cameroon," *Journal of Disaster Risk Studies*, **1**, pp 600-617, **(2009)**.

[27] C.E. Suh, R.S.J. Sparks, J.G. Fitton, S.N. Ayonghe, C. Annen, R. Nana and A. Luckman, "The 1999 and 2000 eruptions of Mount Cameroon: eruption behavior and petrochemistry of lava," *Bulletin of Volcanology*, **65**, pp 267–28, **(2003)**.

[28] L.F. Fombe and J.M. Molombe, "Hydro-geomorphological implications of uncontrolled settlements in Limbe, Cameroon," *International Review of Social Sciences*, **4**, pp 169-183, **(2015)**.

[29] E.O. Longe, "Groundwater resources potential in the Coastal Plain Sands Aquifers, Lagos, Nigeria," *Research Journal of Environmental and Earth Sciences*, **3**, pp 1–7, **(2011)**.

[30] A.E. Djieto Lordon, C.M. Agyingi, V.E. Manga, N.N. Bukalo and E.T Beka, "Geo-electrical and borehole investigation of groundwater in some basalts on the South-Eastern Flank of Mount Cameroon, West Africa," *Journal of Water Resource and Protection*, **9**, pp 1526-1546, **(2017)**.

[31] D.C. Howell, "Méthodes statistiques en sciences humaines," Liège, Belgique : De Boeck Université, **(1999)**.

[32] American Public Health Association (APHA), "Standard methods for the examination of water and wastewater," 20th edn. Washington DC, USA: APHA, **(1998)**.

(This work is licensed under a Creative Commons Attribution 4.0 International License.)

International Journal of Engineering Research & Technology (IJERT)
ISSN: 2278-0181
Vol. 9 Issue 11, November-2020

[33] R. Revelle, "Criteria for recognition of sea water in ground water," *Transactions of American Geophysical Union*, 22, 593–597, **(1941)**.
[34] C. Chatterji, M. Raziuddin, "Determination of water quality index (WQI) of a degraded river in Asanol Industrial area, Raniganj, Burdwan, West Bengal. *Nature, environment and pollution Technology Journal*, **2**, 181-189, **(2002)**.
[35] Centre Technique du Génie Rural des Eaux et de Forêts (CTGREF),"Evaluation des quantités d'eau nécessaires aux irrigations," Paris, France, Ministère de l'Agriculture, **(1979)**.
[36] N. Dörfliger, S. Schomburgk, M. Bouzit, V. Petit, Y. Caballero, P. Durst, O. Douez, M. Chatelier, N. Croiset and N. Surdyk, "Montée du niveau marin induite par le changement climatique: conséquences sur l'intrusion saline dans les aquifères côtiers en Métropole," Orléans, France: BRGM, **(2011)**.
[37] F. Guelemo, "Activités du projet de reconstruction de la péninsule de Bakassi au Cameroun,". Buéa, Cameroun : MINADER, **(2019).**
[38] A. Blivi, "Erosion dans le Golfe de Guinée en Afrique de l'Ouest : exemple du Togo," Lomé, Togo : Centre de Gestion Intégrée du Littoral et de l'Environnement, **(2002)**.
[39] J. Abe, G.H.C. N'doufou, K.E. Konan, K.S. Yao and S.B. Bamba, "Relations entre les points critiques d'érosion et le transit littoral en Côte d'Ivoire," *Africa Geoscience Review*. **21**, pp 1-14, **(2014).**
[40] B. Barry, "Sécheresse et modification des ressources hydriques en basse Casamance. Conséquences pour le milieu naturel et son aménagement," ORSTOM, Dakar/Paris, **(1988).**
[41] B. Diawara, "Impact d'un barrage anti-sel sur la dynamique de la nappe superficielle d'un bas-fond," ORSTOM, CDRO-Dakar, **(1988)**.
[42] K. Furukawa, E. Wolanski and H. Mueller, "Currents and sediment transport in mangrove forest," *Estuarine Coastal and Shelf Sciences*. **44**, 301-310, **(1997)**.
[43] A.J. Tymbery, G.D. Kay, R.G Doupe, G.J. Partridge and H.C. Norman, "The Potential of a salt-tolerant plant (*Distichlis spicata*) to treat effluent from inland saline aquaculture and provide livestock feed on salt-affected farmland," *Science of the Total Environment*, **446**, 192–201, **(2019)**.

(This work is licensed under a Creative Commons Attribution 4.0 International License.)